Photorefractive properties of $LiNbO_3$ crystals doped by copper diffusion

K. Peithmann,* J. Hukriede, K. Buse, and E. Krätzig
Fachbereich Physik, Universität Osnabrück, D-49069 Osnabrück, Germany
(Received 1 June 1999)

Lithium niobate volume crystals (up to 1 mm thick) are doped by indiffusion of thin layers of evaporated copper. The obtained samples are investigated by conventional electrical and holographic methods. Saturation values Δn_s of the refractive-index changes, bulk-photovoltaic current densities j_{phv}, and photoconductivities σ_{ph} are measured utilizing samples with copper concentrations in the range $(2.2-145)\times 10^{24}$ m^{-3}. Comparison with experimental data for melt-doped lithium niobate shows that the photorefractive properties do not depend on the doping technique. Another important outcome is that the refractive-index changes saturate at 7×10^{-4} (ordinary light polarization, green light) for copper concentrations larger than 60×10^{24} m^{-3}. This is caused by a strong increase of the photoconductivity for high doping levels.

I. INTRODUCTION

Lithium niobate ($LiNbO_3$) is a promising photorefractive material for applications in the fields of, e.g., wavelength filters[1] and holographic data storage.[2–5] The photorefractive effect is based on the buildup of electronic space-charge fields upon inhomogeneous illumination. These fields modulate the refractive index via the electrooptic effect. Often $LiNbO_3$ crystals are doped with iron,[6,7] which occurs in $LiNbO_3$ in the valence states Fe^{2+} and Fe^{3+}. These ions act as sources and traps of electrons. Space-charge fields and refractive-index changes are supposed to increase linearly with the Fe^{3+} concentration.[8–10] Anyhow, recent experiments show that the saturation values of the refractive-index changes Δn_s are limited, even for highly doped samples. The reason is a strong increase of the photoconductivity.[10] Furthermore, the dark conductivity rises also with higher iron content which is disadvantageous, too. It is an open question whether these detrimental effects can be avoided by doping with other elements.

Copper doping might be an alternative that we want to investigate. The growth of $LiNbO_3$ crystals doped with different amounts of copper by adding CuO to the melt for this purpose is timeconsuming and expensive. We use diffusion-doped samples. It is known that the diffusion constant of copper in $LiNbO_3$ is more than 500 times larger than that of iron under the same conditions.[11,12] Therefore, in the present contribution diffusion-doped $LiNbO_3$ volume crystals are investigated. For this purpose, thin layers of copper are evaporated on undoped $LiNbO_3$ wafers, and subsequently the copper is indiffused by keeping the crystals at high temperature for some time. Diffusion doping allowed us to prepare a large number of $LiNbO_3$ samples with different amounts of copper and to explore carefully the magnitude of the refractive-index changes as a function of the doping level.

Copper appears in $LiNbO_3$ also in two different valence states (Cu^+ and Cu^{2+}). Former investigations with melt-doped $LiNbO_3$:Cu samples showed that the photorefractive effect and the charge-transport processes can be well understood in terms of the one-center model:[13] Electrons from Cu^+ impurities are excited into the conduction band by green or blue light. They are redistributed and finally trapped by Cu^{2+} centers acting as empty traps. The bulk-photovoltaic effect is the main charge-driving force.[14] The one-center model yields the relations $j_{phv} \propto c_{Cu^+} I$, $\sigma_{ph} \propto (c_{Cu^+}/c_{Cu^{2+}})I$, and $\Delta n_s \propto c_{Cu^{2+}}$, where j_{phv} is the bulk-photovoltaic current density, σ_{ph} is the photoconductivity, Δn_s is the saturation value of the refractive-index changes, c_{Cu^+} and $c_{Cu^{2+}}$ are the concentrations of filled and empty traps, respectively, and I is the averaged light intensity in the crystal.

To enhance, e.g., the storage capacity of $LiNbO_3$:Cu, large values of Δn_s are desired.[15] Large total copper concentrations $c_{Cu} = c_{Cu^+} + c_{Cu^{2+}}$ are required to provide a sufficient concentration $c_{Cu^{2+}}$ even for reduced samples. Here, we present experimental data of the photorefractive properties of $LiNbO_3$:Cu, obtained for a wide range of doping concentrations c_{Cu}. Absorption spectra and the relevant photorefractive properties Δn_s, j_{phv}, and σ_{ph} are measured in these diffusion-fabricated samples, and, for comparison, in some crystals where CuO has been added to the melt during crystal growth.

II. EXPERIMENTAL METHODS

A. Samples

Pieces of two *x*-cut 3'' $LiNbO_3$ wafers, purchased from Crystal Technology (either 1 mm or 0.5 mm thick), are prepared [size about $z\times y = 8\times 5$ mm^2, see Fig. 1(a)]. In a second step, thin copper layers of various thickness are deposited onto the top face of the samples. Up to 715 nm-thick copper layers are employed [Fig. 1(b)]. Then the crystals are wrapped into platinum foil and annealed at 1000°C for 100 h in air. Finally, the slabs are cut into three or four pieces [Fig. 1(c)]: The largest piece (surface size about 5×4 mm) is optically investigated. In some cases repolishing of the surfaces after the annealing treatment is necessary. A list of these samples is given in Table I. Additionally, one smaller crystal is prepared [indiffusion of a 455 nm copper layer, thickness of only 0.8 mm, Fig. 1(d)]. Both *z* faces of this small sample are polished to optical quality.

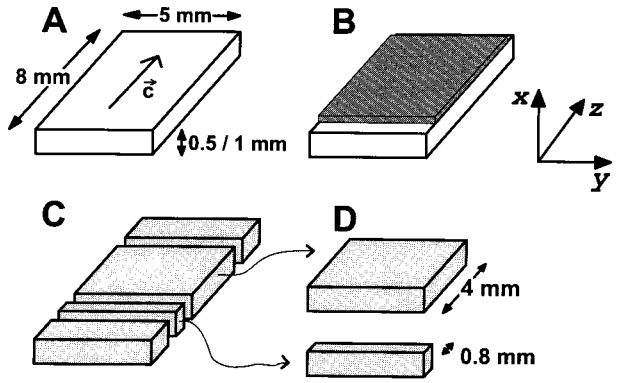

FIG. 1. Crystal fabrication process. (a) Piece of a $LiNbO_3$ wafer, cut from a 3'' crystal, either 1 mm or 0.5 mm thick. (b) A thin layer of copper (thickness up to 715 nm) is deposited onto the top surface. (c) The layer is diffused into the sample, which is then cut into three or (as shown here) four pieces. (d) The prepared samples have dimensions of $5\times4\times1(0.5)$ mm^3. One very small sample is also cut (thickness 0.8 mm).

B. Absorption measurements

Absorption spectra in the visible and infrared wavelength region ($400\ \text{nm}<\lambda<1300\ \text{nm}$) are measured utilizing a CARY 17D spectrometer. The absorption constants $\alpha^{o}_{477\ \text{nm}}$ and $\alpha^{o}_{1040\ \text{nm}}$ yield the concentrations of Cu^{+} and Cu^{2+} ions according to the relations[13,16]

$$c_{Cu^{+}}=2.0\times10^{21}\ \text{m}^{-2}\alpha^{o}_{477\ \text{nm}}, \tag{1}$$

$$c_{Cu^{2+}}=6.8\times10^{22}\ \text{m}^{-2}\alpha^{o}_{1040\ \text{nm}}. \tag{2}$$

Additionally, some spatially resolved absorption measurements are performed using ordinarily polarized, focused laser light ($\lambda=477$ nm, focus diameter of about 50 μm). Our specially prepared thin sample [see Fig. 1(d)] is mounted on a motor-driven translation stage. The sample is moved along the x direction through the focus, and the intensity of the transmitted light is measured. From these data, the dependence of the absorption coefficient $\alpha^{o}_{477\ \text{nm}}$ on the crystal depth x is deduced, i.e., the homogeneity of the Cu indiffusion is checked.

TABLE I. Notation, thickness of the deposited copper layer, and total copper concentration c_{Cu} of the investigated $LiNbO_3$ crystals, deduced from the absorption spectrum or calculated from the Cu-layer thickness. The first number of the notation refers to the crystal boule, the second number enumerates the pieces that have been prepared. Additionally, the investigated samples where CuO was added to the melt are listed, too.

Notation	Cu-layer Thickness (nm)	c_{Cu} (10^{24}m^{-3}) By absorption	By layer thickness
JK17-1, 2, 3		5.3	
JK50-1, 2, 3	65	7.1	5.4
JK100-1, 2, 3	130	14	11
JK200-1, 2, 3	260	31	22
JK350-1, 2, 3	455	55	38
JK500-1, 2, 3	650	75	54
JK400-1, 2, 3	520	106	86
JK550-1, 2, 3	715	145	120
727-17, 18, 19		2.2	
728-5, 8, 14, 32		12	
730-11, 12, 13, 14		72	

The concentration ratio $c_{Cu^{+}}/c_{Cu^{2+}}$ is varied by additional annealing treatments in an argon (for reduction) or oxygen (for oxidation) gas atmosphere.[7,17] For our investigation, we prepare always three crystals with the same total amount of copper, but different ratios $c_{Cu^{+}}/c_{Cu^{2+}}$ varying in the range from 0.03 up to 1.

C. Holographic characterization

Holographic experiments are carried out using a standard two-beam-interference setup (for details see Ref. 10). Light of an argon-ion laser (wavelength $\lambda=514$ nm, ordinary polarization, light intensity up to 1 kW m^{-2}) is used to write one hologram (fringe spacing $\Lambda=1.2$ μm). Alternatively, four holograms are written, which are superimposed by angular multiplexing. In these experiments the technique of incremental recording with active phase locking is utilized.[18–20] Recording beams of equal intensity are used in all cases in order to minimize dynamic effects arising from self diffraction.[21] After waiting until saturation is reached, the obtained diffraction efficiency η is measured by blocking one of the recording beams. The remaining beam is diffracted, and the intensities of transmitted (I_t) and diffracted beam (I_d) are measured. The diffraction efficiency η is calculated using $\eta=I_d/(I_d+I_t)$. In the case of four superimposed holograms, rocking curves $\eta(\vartheta)$ are measured (ϑ: rotational angle of the sample). This takes longer than a single reconstruction of one hologram. Thus the light intensity is lowered by a factor of 100 to avoid erasure effects during reconstruction. From these measurements, the saturation values of the refractive-index changes Δn_s can be deduced, using Kogelnik's formula[22]

$$\eta=\sin^2\left(\frac{\pi\Delta n d}{\lambda\cos\theta}\right), \tag{3}$$

where λ is the vacuum light wavelength, θ the beam angle between the propagation direction of the light and the surface normal inside the sample, and d the thickness of the crystal. In the case of superposition of four holograms of equal strength, the refractive-index change $\Delta n_{s,1}$ of one of the holograms is measured. This yields the saturation value of the refractive-index change for a single hologram via $\Delta n_s=4\times\Delta n_{s,1}$, which has been checked for several samples.

The photoconductivity σ_{ph} is obtained from the time constants of hologram erasure. A third laser beam ($\lambda=514$ nm, ordinary polarization) is used for off-Bragg erasure to avoid any self-enhancement effects. In our experiments ordinarily polarized HeNe-laser light ($\lambda=633$ nm) is used for readout of the holograms. All measurements are carried out under short-circuited conditions that are achieved by contacting the y and z surfaces of the samples with silver-paste electrodes.

Two different techniques for processing of the experimental results are employed: For samples that fulfill the condition $\alpha^{o}_{514\ \text{nm}}d<1$ an averaged light intensity I in the sample

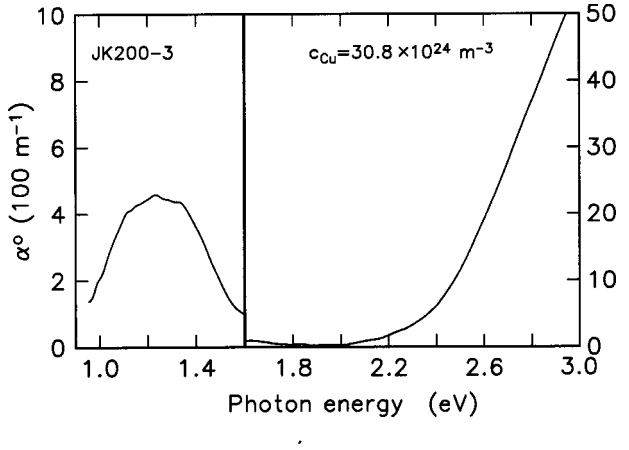

FIG. 2. Absorption coefficient α^o versus photon energy for ordinarily polarized light.

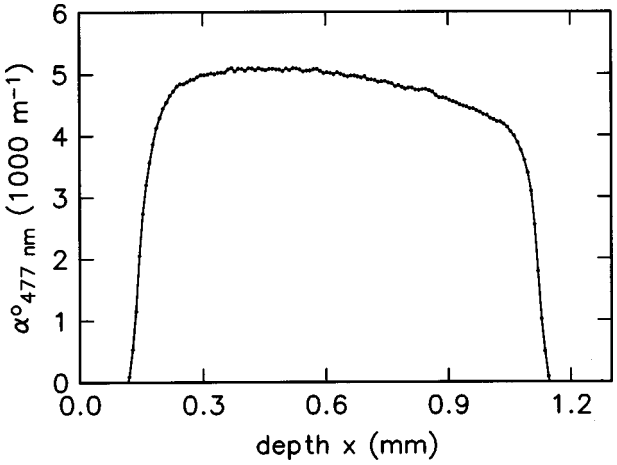

FIG. 3. Absorption coefficient $\alpha^o_{477\,nm}$ versus crystal depth x.

is calculated using $I=I_{in}(1-R)(\alpha^o_{514\,nm}d)^{-1}[1-\exp(-\alpha^o_{514\,nm}d)][1-R\exp(\alpha^o_{514\,nm}d)]^{-1}$ (R denotes the reflectivity, and I_{in} the intensity of the incident light), taking into account absorption and reflection losses. The decay can be described by a monoexponental law $\Delta n(t)=\Delta n_0\exp(-t/\tau)$, where $\Delta n_0=\Delta n(t=0)$ denotes the initial refractive-index change and τ the Maxwell time. From τ we deduce the photoconductivity via $\sigma_{ph}=\epsilon\epsilon_0/\tau$ ($\epsilon=28$ is the dielectric constant,[23] and ϵ_0 the permittivity of free space).

Some crystals exceed the condition $\alpha^o_{514\,nm}d<1$. In this case a monoexponential approximation of $\Delta n(t)$ is not applicable;[24] the influence of the decreasing light intensity along the x direction has to be considered. We solve the coupled-wave equations[22] numerically and calculate σ_{ph} from the τ_{front} at the front surface of the crystal via $\sigma_{ph}=\epsilon\epsilon_0/\tau_{front}$, corresponding to the value $I=(1-R)I_{in}$ for the light intensity.[24]

Bulk-photovoltaic current densities are measured conventionally. The samples are homogeneously illuminated with ordinarily polarized green light ($\lambda=514$ nm, a Xenon arc lamp in combination with a grating monochromator). The z surfaces of the samples are again contacted with silver paste and connected to a high-sensitive electrometer, which detects the photovoltaic current. For a detailed description of this setup see Ref. 25.

III. EXPERIMENTAL RESULTS

A. Samples fabricated by copper indiffusion

Various samples with different copper contents are fabricated. The color of the obtained crystals is brown-orange, quite similar to the color of the samples grown with CuO added to the melt. To quantify this, absorption spectra are measured. In Fig. 2, the absorption spectrum of sample JK200-3 is shown. An absorption band at 1.2 eV (1040 nm) appears, and for a photon energy of more than 2.2 eV the absorption rises again. This spectrum looks as the spectra of conventionally prepared samples.[13] Evaluating these spectra as described above [see Eqs. (1) and (2)], the entire concentration of copper $c_{Cu}=c_{Cu^+}+c_{Cu^{2+}}$ is determined for each sample. The obtained c_{Cu} is found to be independent of the annealing state of the crystal, i.e., of the concentration ratio $c_{Cu^+}/c_{Cu^{2+}}$. Additionally, the total amount of copper in the material is directly calculated using the known thickness of the deposited copper layer and supposing complete indiffusion. Table I summarizes the obtained results.

To check whether a homogeneous distribution of copper through the crystal volume is reached, we measure the absorption coefficient $\alpha^o_{477\,nm}$ as a function of the crystal depth, using the small crystal slab and a focused light beam. The result is shown in Fig. 3. A decrease of the absorption of about 20% with increasing depth occurs.

B. Saturation values of the refractive-index changes

Our results of the saturation values of the refractive-index changes Δn_o for various traps densities $c_{Cu^{2+}}$ are presented in Fig. 4. Three outcomes are noteworthy: (a) The obtained Δn_s is limited. No values above $\Delta n_{s,\,max}=7\times10^{-4}$ can be reached, even for high concentrations $c_{Cu^{2+}}$. For very high contents of empty traps even a decrease of Δn_s is observed. (b) A linear dependence $\Delta n_s\propto c_{Cu^{2+}}$ is found to be correct only for very small values of $c_{Cu^{2+}}$ up to 10×10^{24} m^{-3}. In

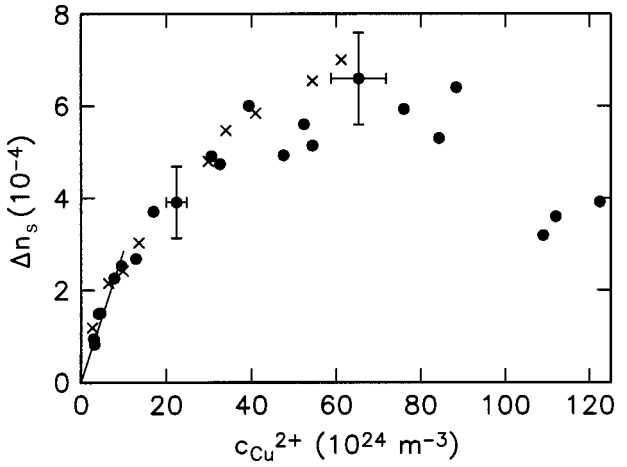

FIG. 4. Saturation values of the refractive-index changes Δn_s versus trap concentration $c_{Cu^{2+}}$ for green light ($\lambda=514$ nm), measured for the diffusion-doped samples (dots) and for the crystals doped conventionally during growth (crosses). A linear dependence $\Delta n_s\propto c_{Cu^{2+}}$ is observed in the range $0<c_{Cu^{2+}}<10^{24}$ m^{-3}; the solid line is a linear fit.

this region we obtain $\Delta n_s / c_{Cu^{2+}} = 2.9 \times 10^{-29}$ m^3. For larger concentrations, Δn_s grows slower, and for very large values of $c_{Cu^{2+}}$, a decrease of the saturation values is observed. (c) The values of Δn_s are independent of the crystal fabrication process; the diffusion-made samples show within the measuring accuracy the same Δn_s as the conventionally doped crystals.

C. Bulk-photovoltaic effect

Bulk-photovoltaic currents are measured for different light intensities and concentrations c_{Cu^+} of filled traps. The results for a medium-doped sample (JK200) are shown in Fig. 5. The first plot reveals that the bulk-photovoltaic current density j_{phv} grows linearly with increasing light intensity I. Part (b) of Fig. 5 shows that the ratio j_{phv}/I depends linearly on the concentration c_{Cu^+}, as predicted by the one-center model. These dependences are carefully checked for all investigated samples, and they are found to be valid even for samples of the highest copper content. Finally, we calculate the bulk-photovoltaic coefficient $\beta^* = j_{phv}/(c_{Cu^+} I)$. The dependence of β^* on the entire copper concentration in the crystal is shown in Fig. 5(c). In this figure, the results for our diffusion-fabricated samples are marked by dots, and the values obtained using the conventional-grown crystals are indicated by crosses. Two outcomes are remarkable: (a) An increase of c_{Cu} causes an enhancement of β^*. In the investigated range (from $c_{Cu} = 2.2 \times 10^{24}$ m^{-3} up to an entire copper content of $c_{Cu} = 145 \times 10^{24}$ m^{-3}) the coefficient β^* grows by a factor of about 3. (b) No significant difference is found between the results obtained with diffusion- and melt-doped samples.

D. Photoconductivity

In this section our results for the photoconductivity σ_{ph} are presented, using the samples JK200. Figure 6(a) shows the dependence of σ_{ph} on light intensity I. A linear relation is found. The second part in Fig. 6 reveals that the ratio σ_{ph}/I depends linearly on the concentration ratio of filled and empty traps, $c_{Cu^+}/c_{Cu^{2+}}$. For all investigated samples we confirm these linear dependences, using light intensities up to 600 Wm^{-2}. As the last step, we calculate the specific photoconductivity as the ratio $\sigma_{ph}/[(c_{Cu^+}/c_{Cu^{2+}})I]$. The dependence of this parameter on the entire content of copper c_{Cu} is shown in Fig. 6(c). Two interesting features are obvious: (a) A very strong increase of the specific photoconductivity is found. It grows in the investigated range by a factor of about 40. (b) Within the measuring accuracy, the obtained values are independent of the crystal-production process.

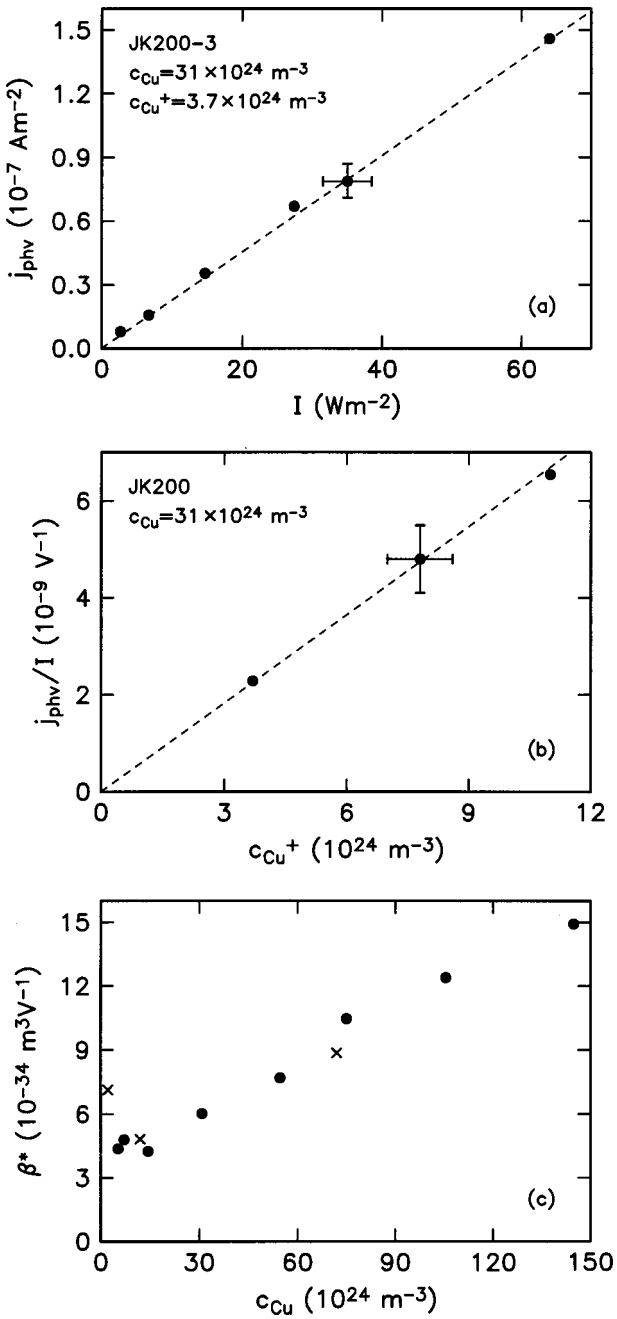

FIG. 5. Measured data (symbols) and linear fits (dashed lines) of: (a) Bulk photovoltaic current density j_{phv} versus light intensity I for $\lambda = 514$ nm, measured with sample JK200-3. (b) Ratio j_{phv}/I versus concentration c_{Cu^+} of filled traps for the crystals JK200. (c) Specific photovoltaic coefficient $\beta^* = (j_{phv}/I)/c_{Cu^+}$ versus entire copper concentration c_{Cu} for diffusion-fabricated samples (dots) and for crystals doped conventionally during growth (crosses).

IV. DISCUSSION

Diffusion of evaporated copper layers into commercially available $LiNbO_3$ wafers is an easy way to produce doped volume material. The resulting samples have similar photorefractive properties as crystals fabricated by adding CuO to the melt: The color and the absorption spectrum correspond to those of conventional $LiNbO_3$:Cu, and bulk-photovoltaic coefficients and specific photoconductivities are equal. In moderate diffusion times (100 h) a quite good homogeneity of the copper distribution in the 1 mm-thick material is reached (see Fig. 3); the value of $\alpha^{o}_{477\,nm}$ for one sample varies in the range of only 20%. The long annealing time of 100 h rules out that a changed $c_{Cu^+}/c_{Cu^{2+}}$ concentration ratio is the reason of the small remaining absorption inhomogeneity. However, this variation of c_{Cu} has no significant influence on our experimental results, which has been checked by turning the crystals and illuminating them from the other side in our holographic setup. Additionally, the changes of the light intensity $I(x)$ within the sample due to absorption are much larger than the change of c_{Cu}. Evapo-

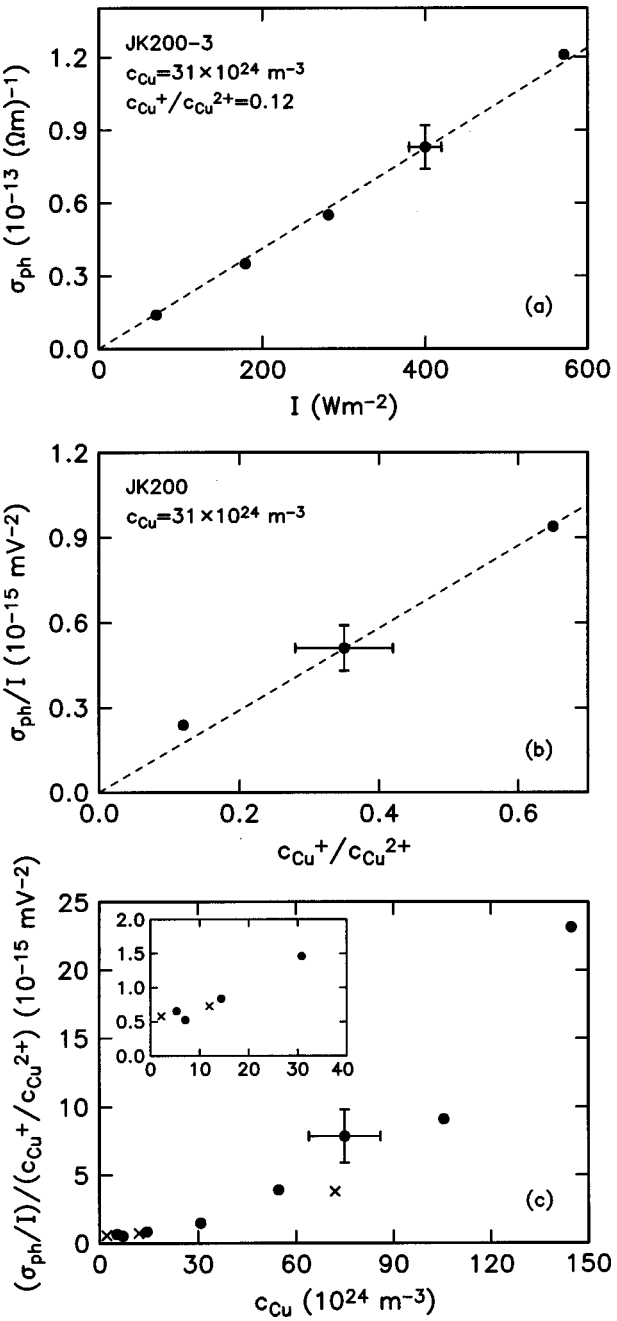

FIG. 6. Measured data (symbols) and linear fits (dashed lines) of: (a) Photoconductivity σ_{ph} versus light intensity I (sample JK200-3). (b) Ratio σ_{ph}/I versus $c_{Cu^+}/c_{Cu^{2+}}$ for the crystals JK200. (c) Specific photoconductivity $(\sigma_{ph}/I)/(c_{Cu^+}/c_{Cu^{2+}})$ versus entire copper concentration c_{Cu} for diffusion-fabricated samples (dots) and for crystals doped conventionally during growth (crosses).

rating copper onto both surfaces of the wafer may improve the homogeneity further and may allow fabrication of samples thicker than 1 mm. So for photorefractive applications of $LiNbO_3$:Cu, our technique might be an easy, practicable, and inexpensive way to provide samples.

Comparing the values for the copper content c_{Cu} measured by absorption spectra and calculated from the deposited copper layer thickness, we find a mismatch of up to 30%. The mismatch occurs for all samples that we have investigated. This may arise from difficulties in estimating our evaporated layer thickness, but also uncertainties in the factors $c_{Cu^+}/\alpha^{o}_{477\ nm}$ and $c_{Cu^{2+}}/\alpha^{o}_{1040\ nm}$ may contribute. Further investigations, such as EPR or neutron-activation experiments are supposed to elucidate this topic. But it should be pointed out that the doping level, controlled by depositing a certain layer thickness, can be adjusted very carefully. This is an advantage compared to the conventional method, which suffers from the fact that the distribution factor of copper for melt growth of $LiNbO_3$:Cu is different from one.[26] This causes problems regarding adjustment of the desired content of c_{Cu} in the samples and regarding the doping homogeneity. In our investigation, we always use the copper concentrations c_{Cu} deduced from optical absorption measurements. This allows the comparison of photorefractive properties of samples prepared by different doping techniques.

We show that the saturation values of the refractive-index changes Δn_s depend linearly on the trap concentration $c_{Cu^{2+}}$ only for values smaller than 10×10^{24} m^{-3}. Our results match previously published data [$\Delta n_s/c_{Cu^{2+}}=2.6\times10^{-29}$ m^3, (Ref. 27)] which were measured with blue light ($\lambda=488$ nm). Furthermore, we can estimate $\Delta n_s/c_{Cu^{2+}}$ from our values for β^* and $\sigma_{ph}/[I(c_{Cu^+}/c_{Cu^{2+}})]=f$ using $|\Delta n_s|=(1/2)n^3rE_{SC}$ and $E_{SC}=E_{phv}=j_{phv}/\sigma_{ph}=\beta^* c_{Cu^+}I/[fI(c_{Cu^+}/c_{Cu^{2+}})]$, which yields $\Delta n_s=[(1/2)n^3r\beta^*/f]c_{Cu^{2+}}$ ($n=2.33$ (Ref. 28) is the refractive index at $\lambda=514$ nm, and $r=10$ pmV^{-1} (Ref. 29) is the electro-optic coefficient). For the samples JK17 ($c_{Cu}=5.3\times10^{24}$ m^{-3}) we have $\beta^*=4.4\times10^{-34}$ m^{3}V^{-1} and $f=6.5\times10^{-16}$ mV^{-2} which gives $\Delta n_s/c_{Cu^{2+}}=4.3\times10^{-29}$ m^3. This result agrees quite good with our measured value 2.9×10^{-29} m^3.

The refractive-index changes are limited for higher trap concentrations ($c_{Cu}>60\times10^{24}$ m^{-3}); saturation values larger than $\Delta n_s=7.0\times10^{-4}$ cannot be reached. This limit is exactly the same than that of iron-doped $LiNbO_3$.[10] But, contrary to $LiNbO_3$:Fe, a three times higher doping level of about 60×10^{24} m^{-3} is necessary to obtain the maximum Δn_s. Anyhow, copper doping does not yield larger holographic storage capacities of $LiNbO_3$ than iron doping. Perhaps the measured upper limit of the refractive-index changes is a generally valid value, independent from the photorefractive center involved. Investigation of crystals doped with other elements, e.g., Cr or Mn, could answer this question. The limitation of Δn_s is caused by a very strong increase of the photoconductivity. This increase was also observed in the case of iron-doped $LiNbO_3$. The high photoconductivity short-circuits the space-charge fields. This overcompensates the increase of the specific bulk-photovoltaic coefficient. The reason for the boost of σ_{ph} should be further investigated: Properties like absorption cross section, electron mobility, or electron lifetime in the conduction band might be changed in the highly doped material.

V. CONCLUSIONS

Doping of $LiNbO_3$ by in-diffusion of thin copper layers is an easy way to produce photorefractive samples with a desired copper concentration. Our results clearly indicate that the properties are comparable to that of conventionally

doped crystals where copper was added to the melt during their growth; this is shown for saturation values of refractive-index changes Δn_s, bulk-photovoltaic current densities j_{phv}, and photoconductivities σ_{ph}. We find a strong increase of the specific photoconductivity with increasing copper content. This important result leads to the conclusion that refractive-index changes Δn_s are limited to values smaller than 7×10^{-4} (ordinarily polarized light, $\lambda=514$ nm), as in the case of iron-doped samples.

ACKNOWLEDGMENTS

Valuable help by E. Bondarenko and S. Schwalenberg is highly appreciated. Financial support by the Deutsche Forschungsgemeinschaft (SFB 225) is gratefully acknowledged.

*Electronic address: konrad.peithmann@physik.uni-osnabrueck.de

[1] S. Breer, H. Vogt, I. Nee, and K. Buse, Electron. Lett. **34**, 2419 (1999).
[2] F. S. Chen, J. T. LaMacchia, and D. B. Fraser, Appl. Phys. Lett. **13**, 223 (1968).
[3] A. Ashkin, G. D. Boyd, J. M. Dziedzic, R. G. Smith, A. A. Ballman, J. J. Levinstein, and K. Nassau, Appl. Phys. Lett. **9**, 72 (1966).
[4] D. Psaltis and F. Mok, Sci. Am. **273(5)**, 70 (1995).
[5] R. M. Shelby, J. A. Hoffnagle, G. W. Burr, C. M. Jefferson, M.-P. Bernal, H. Coufal, R. K. Grygier, H. Guenther, R. M. Macfarlane, and G. T. Sincerbox, Opt. Lett. **22**, 1509 (1997).
[6] H. Kurz, E. Krätzig, W. Keune, H. Engelmann, U. Gonser, B. Dischler, and A. Räuber, Appl. Phys. **12**, 355 (1977).
[7] J. J. Amodei, W. Phillips, and D. L. Staebler, Appl. Opt. **11**, 390 (1972).
[8] R. Sommerfeldt, L. Holtmann, E. Krätzig, and B. C. Grabmaier, Phys. Status Solidi A **106**, 89 (1988).
[9] K. Buse, Appl. Phys. B: Lasers Opt. **64**, 391 (1997).
[10] K. Peithmann, A. Wiebrock, and K. Buse, Appl. Phys. B: Lasers Opt. **68**, 777 (1999).
[11] J. Hukriede, B. Gather, D. Kip, and E. Krätzig, Phys. Status Solidi A **172**, R3 (1999).
[12] D. Kip, B. Gather, H. Bendig, and E. Krätzig, Phys. Status Solidi A **139**, 241 (1993).
[13] E. Krätzig and R. Orlowski, Ferroelectrics **27**, 241 (1980).
[14] A. M. Glass, D. von der Linde, and T. J. Negran, Appl. Phys. Lett. **25**, 233 (1974).
[15] F. H. Mok, G. W. Burr, and D. Psaltis, Opt. Lett. **21**, 896 (1996).
[16] K. Buse, S. Breer, K. Peithmann, S. Kapphan, M. Gao, and E. Krätzig, Phys. Rev. B **56**, 1225 (1997).
[17] G. E. Peterson, A. M. Glass, and T. J. Negran, Appl. Phys. Lett. **19**, 130 (1971).
[18] P. A. M. Dos Santos, L. Cescato, and J. Frejlich, Opt. Lett. **13**, 1014 (1988).
[19] Y. Taketomi, J. E. Ford, H. Sasaki, J. Ma, Y. Fainman, and S. H. Lee, Opt. Lett. **16**, 1774 (1991).
[20] K. Peithmann, A. Wiebrock, and K. Buse, Opt. Lett. **23**, 1927 (1998).
[21] N. V. Kukhtarev, V. B. Markov, S. G. Odoulov, M. S. Soskin, and V. L. Vinetskii, Ferroelectrics **22**, 949 (1979).
[22] H. Kogelnik, Bell Syst. Tech. J. **48**, 2909 (1969).
[23] A. Mansingh and A. Dhar, J. Phys. D **18**, 2059 (1985).
[24] J. Baquedano, M. Carrascosa, L. Arizmendi, and J. M. Cabrera, J. Opt. Soc. Am. B **4**, 309 (1987).
[25] K. Buse, U. van Stevendaal, R. Pankrath, and E. Krätzig, J. Opt. Soc. Am. B **13**, 1461 (1996).
[26] A. Räuber, Mater. Sci. Eng. **7**, 481 (1978).
[27] R. Sommerfeldt, R. A. Rupp, H. Vormann, and E. Krätzig, Phys. Status Solidi A **99**, K15 (1987).
[28] R. S. Weis and T. K. Gaylord, Appl. Phys. A: Solids Surf. **37**, 191 (1985).
[29] K. Onuki, N. Uchida, and T. Saku, J. Opt. Soc. Am. **62**, 1030 (1972).